Journal of Alloys and Compounds 507 (2010) 494–497

Contents lists available at ScienceDirect

Journal of Alloys and Compounds

journal homepage: www.elsevier.com/locate/jallcom

# CVD fabrication of carbon nanotubes on electrodeposited flower-like Fe nanostructures

Saeid Zanganeh[a,e,*], Morteza Torabi[b,e], Amir Kajbafvala[c], Navid Zanganeh[d], M.R. Bayati[b], Roya Molaei[b], H.R. Zargar[b], S.K. Sadrnezhaad[e]

[a] Department of Electrical and Computer Engineering, University of Connecticut, 371 Fairfield Way, U-2157 Storrs, CT 06269-2157, USA
[b] Department of Metallurgy and Materials Engineering, Iran University of Science and Technology, P.O. Box 16845-161, Tehran, Iran
[c] Department of Materials Science and Engineering, North Carolina State University, 911 Partner's Way, Raleigh, NC 27695-7907, USA
[d] Chemical Engineering Department, Amirkabir University of Technology, P.O. Box 15875-4413, Tehran, Iran
[e] Department of Materials Science and Engineering, Center of Excellence for Production of Advanced Materials, Sharif University of Technology, P.O. Box 11365-9466, Tehran, Iran

ARTICLE INFO

*Article history:*
Received 31 March 2010
Received in revised form 30 July 2010
Accepted 30 July 2010
Available online 8 August 2010

*Keywords:*
Nanostructure
Carbon nanotubes
Electrodeposition
Chemical vapor deposition

ABSTRACT

Galvanostatic method was used to electrodeposit Fe nanostructures on platinum electrodes as catalysts. Scanning electron microscopy (SEM) revealed flower-like Fe deposits with high surface area. Carbon nanotubes were grown on flower-like Fe nanostructures by chemical vapor deposition. The structure of the synthesized carbon nanotubes was investigated by scanning electron microscopy, transmission electron microscopy, Raman spectroscopy and X-ray diffraction. According to X-ray diffraction patterns, Fe was the only detected constituent of the deposited coating. The carbon nanotubes had small wall-thickness and wide hollow core.



## 1. Introduction

Carbon nanotubes (CNTs) have tubular structure and graphitic lattice [1]. Due to unique atomic structure, extraordinary mechanical strength, desirable electronic properties [2–4], high material storage capacity for special applications such as drug delivery and optics [5,5-b,5-c,6], CNTs have inspired wide interest in the current nanoscience/nanotechnology progressing versatile fields. CNTs can be produced via carbon arc discharge [7], laser ablation [8], pyrolysis [9,10], chemical vapor deposition (CVD) [11,12] and plasma enhanced chemical vapor deposition [13,14]. CVD seems to be a promising technique because of its low cost, high purity, high yield, simple configuration and flexibility in adjustment of the influential parameters such as temperature and presence of hydrocarbon gases [15] which can be used to control the structure of the CNTs produced [16–18].

A key factor in controlling the growth of CNT by CVD is utilization of a suitable nanosized catalyst. Nanosized metallic catalysts such as iron, cobalt and nickel [19] have been widely reported as nuclei for growth of CNTs by CVD [20,21]. The peculiar ability of the nanosized catalysts to promote the CNT growth is attributed to their catalytic activity of decomposition of carbon feedstock, formation of metastable carbides and subsequent diffusion of carbon atoms and formation of graphitic sheets [22]. Techniques for preparation of the catalysts have therefore become an important issue. Trying to efficiently screen the preparation conditions of CNT catalysts, several studies have used combinatorial approaches involving dry [23,24] and wet [25,26] processes. Galvanostat method is a simple way, requiring shorter times and yielding greater rates.

The latest results obtained about production of flower-like nanostructured Fe catalysts deposited electrochemically on platinum electrodes (as a suitable catalyst for synthesis of carbon nanotubes) are presented in this paper. CVD is used as a convenient way of deposition of CNTs on the flower-like Fe catalyst substrate.

### 2. Experimental procedure

The electrolyte contained 0.1 M $FeSO_4 \cdot 7H_2O$ (99.5%, $M = 278.02\ g\ mol^{-1}$, Merck, Germany) in an aqueous solution of 0.1 M $Na_2SO_4$ (99.99%, $M = 142.04\ g\ mol^{-1}$, Merck, Germany). The platinum sheets were carefully polished and cleaned before the experiments. All the electrochemical processes were carried out in a potentiostat/galvanostat equipment (Autolab PGSTAT30) using a standard three electrode cell. Electrochemical potentials were recorded versus an Ag/AgCl reference electrode. Linear sweep voltammetry was applied in the potential range of −0.1 to −1.8 V vs. Ag/AgCl in order to deposit nanostructured iron on Pt electrode. To understand the mechanism of electrodeposition of iron, different electrochemical measurements including linear sweep voltammetry (LSV), chronopotentiometry and chronoamperometry were carried out on the samples. The morphology of the

* Corresponding author at: Department of Electrical and Computer Engineering, University of Connecticut, 371 Fairfield Way, U-2157 Storrs, CT 06269-2157, USA.
*E-mail address:* SAZ@engr.uconn.edu (S. Zanganeh).

0925-8388/$ – see front matter © 2010 Elsevier B.V. All rights reserved.
doi:10.1016/j.jallcom.2010.07.216

Fe-coated platinum substrates obtained was characterized by a scanning electron microscope (SEM, VEGA, TESCAN) equipped with energy dispersive X-ray (EDX). X-ray diffraction analysis by Philips X'Pert XRD diffractometer using Cu-$K_\alpha$ radiation ($\lambda$ = 1.5405 Å) was used to identify the crystalline structure of the deposited layer. BET was used to investigate the specific surface area of the prepared catalyst (Gemini Micrometrics 2375).

The nanostructured flower-like Fe catalyst obtained via linear sweep voltammetry is utilized to synthesize carbon nanotubes via CVD process. In order to fabricate CNTs on the catalyst, the Fe-coated platinum substrate was placed at the center of a quartz tube reactor heated to about 700 °C under flowing nitrogen/hydrogen (10:1 molar ratio) gas mixture. After reaching to the desired temperature (700 °C), a flow of acetylene ($C_2H_2$) gas was introduced into the reactor with a rate of 60 ml/min for about 30 min. A black coating covered the surface of the catalyst which was analyzed using transmission electron microscope (TEM, Philips CM200), X-ray diffractometer (XRD, Philips X'Pert diffractometer) and Raman spectroscope (Thermo Nicolet).

## 3. Results and discussion

### 3.1. Production of flower-like nanostructured Fe catalyst

Fig. 1A indicates the onset potential of ca −1.0 V vs. Ag/AgCl for iron deposition. No reduction peak can be observed in the figure. It can, therefore, be concluded that the mechanism of the reduction reaction is charge-transfer which is controlled by increasing the potential which culminates at elevated densities of the current.

Transition time ($\tau$) vs. current density measurements can provide valuable information about the reaction mechanism. Fig. 1B represents the Galvanostatic transient for deposition of Fe from the electrolyte at 10 mA/cm$^2$. It shows a sharp peak which relates to the double-layer capacitance at initial part of the curve. This is related to the coalescence of charges on the surface of the Pt electrode. Reduction in the potential right after the initial-part sharp peak corresponds to the charge-transfer processes which occur during the Fe deposition process. This finding is in consistence with the results of linear sweep voltammetry which approved the dominance of charge-transfer processes in deposition of Fe layer. Following the reduction step in the chronopotentiometry diagram (Fig. 1A), the potential changes towards the nobler potential section (∼−1.08002 V vs. Ag/AgCl) which corresponds to the transient stage, slowly increases to −1.028 V vs. Ag/AgCl with the growth continuation. It can, therefore, be concluded that the deposition observed in this system is controllable through charge-transfer mechanism.

For confirmation of the charge-transfer mechanism in the system, chronoamperometric (*I–t* transient) measurements were done at −1.0 V vs. Ag/AgCl. Fig. 1C shows the *I–t* transient curve of the system. As it is clearly seen, the diagram has one well-defined recognizable maximum current (first peak) followed by a sharp fall and subsequent broad noisy peak. Such a particular shape for the *I–t* transient curve clearly shows that a nucleation and growth process is involved in the electrodeposition of Fe and charge-transfer is the rate-limiting process. The oscillations observed in this diagram can be attributed to the instability of the system.

As it is seen in the first stage of the Fe electrodeposition, instabilities such as nucleation and double-layer effect occur. Furthermore, in the galvanostatic process, the stability is reached after about 200 s. A longer deposition time is required for synthesis of a more uniform catalyst layer. About 300 s is, hence, used for this purpose.

The electroactive-type concentration of the solution was changed during the experiment. The changes were, however, not sufficient and the current density decreased very little. Using Pt caused the decrease of the $H_2$ evolution and increase of the cathodic current efficiency. It could, therefore, be expected that the current density is consumed during the ferrous reduction.

X-ray diffraction spectrum of the deposited layer is presented in Fig. 2. The curve shows different peaks attributed to the platinum substrate and the Fe deposited layer. The average crystallite size of the deposited Fe layer was calculated through Scherrer formula

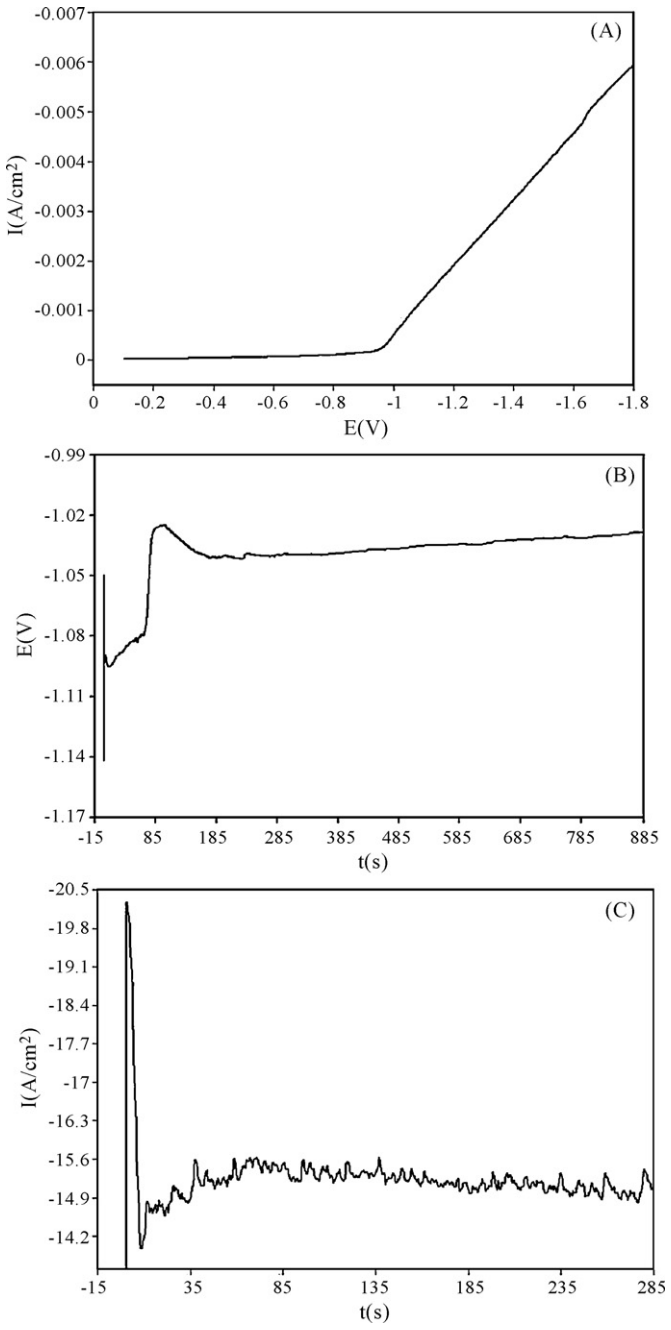


**Fig. 1.** (A) The linear voltammogram related to electrodeposition of iron on platinum substrate in the required potential range from −0.1 to −1.8 V, (B) galvanostatic *E–t* transients for deposition of Fe from electrolyte and (C) potentiostatic *I–t* transients for deposition of Fe from electrolyte.

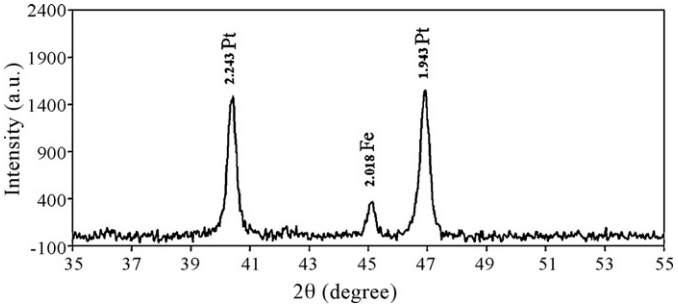


**Fig. 2.** XRD pattern of the deposited Fe on the platinum substrate.

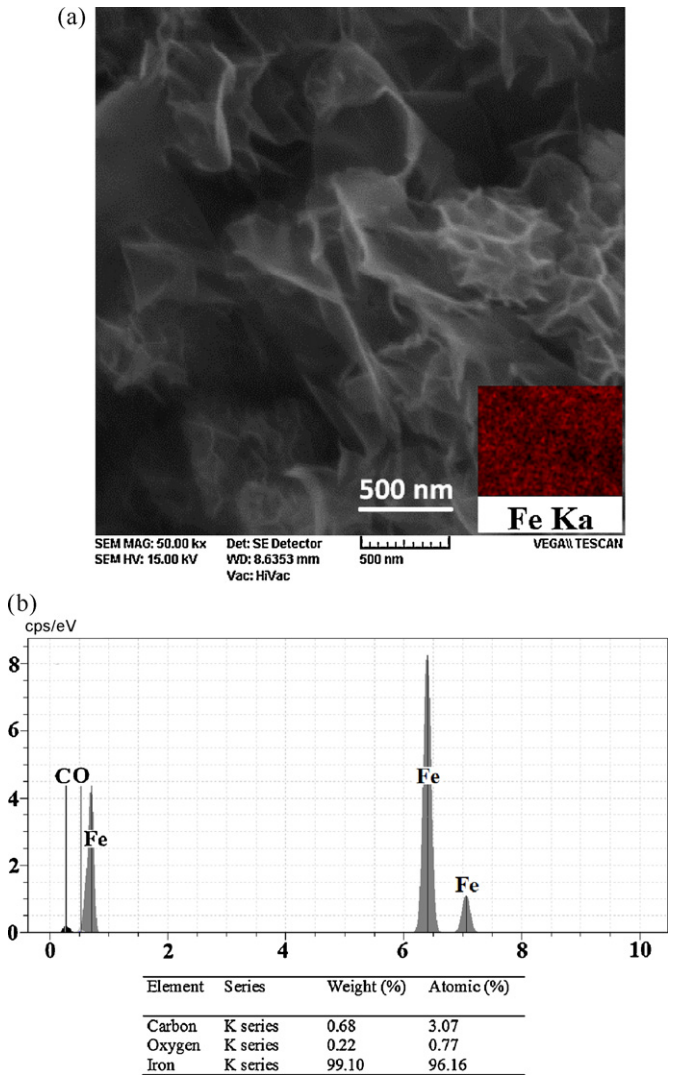


| Element | Series | Weight (%) | Atomic (%) |
|---|---|---|---|
| Carbon | K series | 0.68 | 3.07 |
| Oxygen | K series | 0.22 | 0.77 |
| Iron | K series | 99.10 | 96.16 |

**Fig. 3.** (a) SEM image, Fe mapping and (b) EDS results of the deposited Fe layer.

($d = 0.9\lambda/B\cos\theta$: $d$ is the average crystallite size of the deposited layer, $\lambda$ is the wavelength of Cu-$K_\alpha$ radiation, $B$ is the full width at half maximum intensity of the sharpest Fe peak and $\theta$ is the Bragg angle). The result obtained was ~28.7 nm.

Fig. 3 illustrates the SEM morphology of the nanostructured Fe layer. The layers formed were composed of exfoliated Fe petal-like nanostructures which make a flower-like nanostructure. Elemental mapping reveals homogenous distribution of the Fe atoms. Moreover, the EDS results show that Fe is the major component of the catalyst (99.1 wt%). Oxygen and carbon may be attributed due to contamination of the surface or slight iron oxides. The BET surface area of the Fe catalyst that was synthesized electrochemically is about 287 $m^2/g$. This rather high surface area is a result of the flake-like morphology of the Fe catalyst.

### 3.2. CVD growth of CNTs on flower-like Fe nanostructures

Fig. 4 shows the XRD pattern of the black material obtained on the surface of the catalyst after the CVD process. A strong sharp peak occurs at $2\theta = 25.20$ corresponding to the (0 0 2) reflection of the graphitic carbon deposited on the flower-like Fe nanostructure. XRD results clearly indicate the well graphitized highly pure CNTs fabricated in this research.

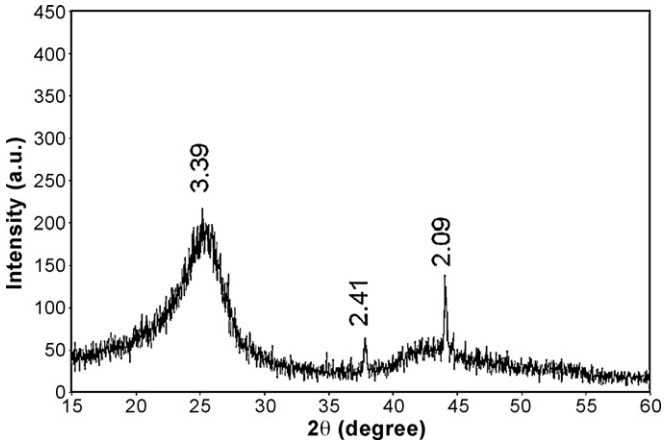


**Fig. 4.** XRD pattern of the CNTs grown on the flower-like Fe nanostructures electrodeposited on platinum electrode.

Transmission electron microscopy (TEM) images of the produced CNTs show a randomly entangled network of long and curved CNTs grown in various diameters between 9 nm and 35 nm which have small wall-thickness and therefore a large inner space (Fig. 5a and b). These wide hollow cores and small wall-thicknesses provide appropriate conditions for transfer through empty nanotube channels and improve the required potential for both storage and drug delivery applications.

High-resolution images of all tubes formed in CVD experiments (Fig. 6) reveal well-ordered graphitic layers grown on the

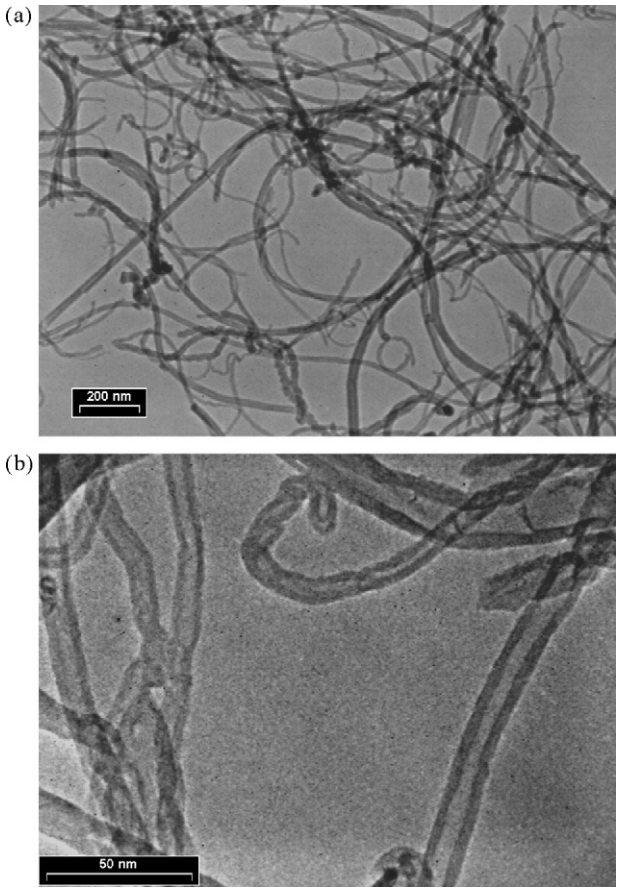


**Fig. 5.** TEM image of the CNTs grown on flower-like Fe nanostructures electrodeposited on platinum electrode by CVD method at (a) lower magnification and (b) higher magnification.

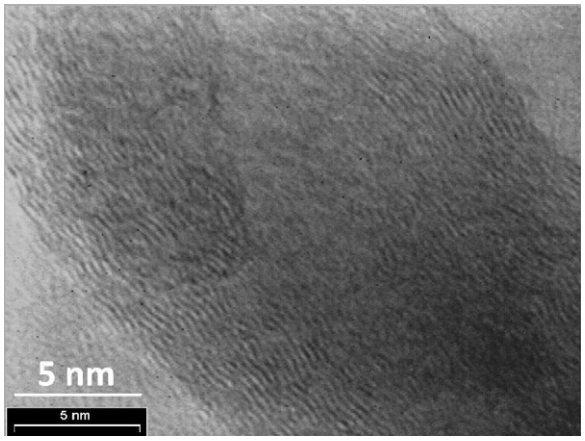


**Fig. 6.** High-resolution TEM image of the synthesized walls of CNTs grown on the Fe nanostructures at 8,500,000 magnification.

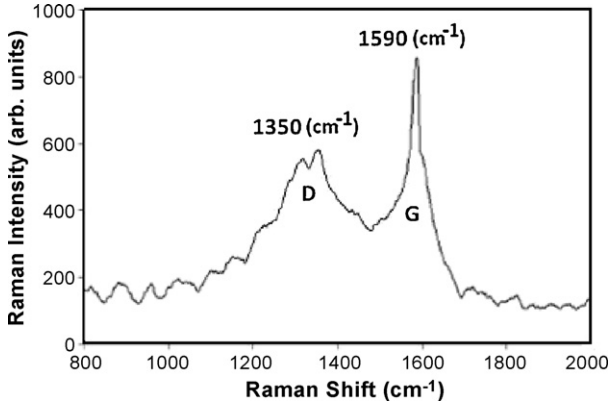


**Fig. 7.** Raman spectroscopy diagram of the CNTs grown on flower-like Fe nanostructure.

Fe nanostructured substrates. Carbon products have hollow structured graphitic sheets on multiwalled carbon nanotubes (MWCNT) which are aligned along the nanotube axis.

Raman spectra can be used to reveal the graphitic nature of the fabricated CNTs (Fig. 7). A G-peak is, therefore, seen at about 1590 $cm^{-1}$ originating mainly from the graphite in plane $E_{2g}$ vibration mode and a D-peak at about 1350 $cm^{-1}$ attributed to a finite particle size effect and/or structural disorder within the carbon sheets. The 1350 $cm^{-1}$ band is not a Raman active mode of the graphene layer. It is generally attributed to the defects in the curved graphene layers, tube ends and staging disorder. The D-band is associated with vibrations of carbon atoms with dangling bonds in plane terminations of the disordered graphite or glassy carbons.

The intensity ratio of $I_D/I_G$ is known to depend on the structural characteristics of CNTs, and is a usual measurement of the graphitic ordering. The $I_D/I_G$ value of the spectrum suggests a defective structure or a lower degree of graphitization in CNT structure. It indicates that the number of $sp^2$-bonded carbon atoms without dangling bonds has increased at the expense of disordered carbon. $sp^2$-bonded carbon is the bonding of carbon atoms in a single graphite layer of perfect hexagonal lattice. Other carbon allotropes made of concentric multiwalled layers of two-dimensional hexagonal carbon lattice such as nanotubes and nanofibers display the same vibration and no other characteristic Raman features. According to the analysis of Kasuye et al. [27], the structure of 1540–1600 $cm^{-1}$ can be understood by z1-folding of the graphite phonon dispersion relation.

## 4. Conclusions

This paper investigates the application of a special shape of iron nanostructures as a catalyst for high-yield preparation of high purity CNTs with desirable nanostructure. Flower-like Fe nanostructure was produced as an appropriate catalyst for preparation of highly pure CNT via electrodeposition from iron sulfate electrolyte on a platinum electrode. The growth mechanisms were administered via linear sweep voltammetry, chronopotentiometry and chronamperometry. It was found that the electrodeposition was charge-transfer controlled. BET confirmed high surface area of the Fe catalyst. Elemental mapping and EDS results showed uniform distribution of Fe in the catalyst with negligible impurities. The structure of the synthesized carbon nanotubes, and flower-like Fe nanostructure were investigated by scanning electron microscopy, transmission electron microscopy, Raman spectroscopy and X-ray diffraction. Using the CVD method, long carbon nanotubes with small wall-thicknesses and wide hollow cores in various diameters between 9 nm and 35 nm were obtained.

## References

[1] S. Iijima, Nature 354 (1991) 56.
[2] M.M. Treacy, T.W. Ebbesen, J.M. Gibson, Nature 381 (1996) 678.
[3] N. Hamada, S. Sawada, A. Oshiyama, Phys. Rev. Lett. 68 (1992) 1579.
[4] K. Harigaya, M. Fujita, Phys. Rev. B 473 (1993) 1656.
[5] (a) D.S. Bethune, C.H. Kiang, M.S. de Urief, G. Gorman, R. Savoy, J. Vazquez, R. Beyers, Nature 363 (1993) 605;
(b) P.D. Kumavor, E. Donkor, B.C. Wang, IEEE J. Sel. Top. Quantum Electron. 12 (2006) 697;
(c) C.B. Nrusingh, J.K. Gamelin, J. Biomed. Opt. 15 (1) (2010) 016012.
[6] P. Singh, Chalcogenide Lett. 7 (2010) 389.
[7] W.K. Maser, E. Muñoz, A.M. Benito, M.T. Martıínez, G.F. de la Fuente, Y. Maniette, E. Anglaret, J.-L. Sauvajol, Chem. Phys. Lett. 292 (1998) 587.
[8] M. Terrones, N. Grobert, J. Olivares, J.P. Zhang, H. Terrones, K. Kordatos, W.K. Hsu, J.P. Hare, P.D. Townsend, K. Prassides, A.K. Cheetham, H.W. Kroto, D.R.M. Walton, Nature 388 (1997) 52.
[9] R. Sen, A. Govindaraj, C.N.R. Rao, Chem. Phys. Lett. 267 (1997) 276.
[10] Z.F. Ren, Z.P. Huang, J.W. Xu, J.H. Wang, P. Bush, M.P. Siegel, P.N. Provencio, Science 282 (1998) 1105.
[11] X. Ma, E.G. Wang, W. Zhou, D.A. Jefferson, J. Chen, S. Deng, N. Xu, J. Yuan, Appl. Phys. Lett. 75 (1999) 3105.
[12] W.Z. Li, S.S. Xie, L.X. Quain, B.H. Chang, B.S. Zou, W.Y. Zhou, R.A. Zhao, G. Wang, Science 274 (1996) 1701.
[13] S. Fan, M.G. Chapline, N.R. Franklin, T.W. Tombler, A.M. Cassen, H. Dai, Science 283 (1999) 512.
[14] C.J. Lee, J. Park, Y. Huh, J.Y. Lee, Chem. Phys. Lett. 343 (2001) 33.
[15] P. Nikolaev, M.J. Bronikowski, R. Kelley Bradley, F. Rohmund, D.T. Colbert, K.A. Smith, R.E. Smalley, Chem. Phys. Lett. 313 (1999) 91.
[16] Y. Murakami, S. Chiashi, Y. Miyauchi, M. Hu, M. Ogura, T. Okubo, S. Maruyama, Chem. Phys. Lett. 385 (2004) 298.
[17] K. Hata, D.N. Futaba, K. Mizuno, T. Namai, M. Yumura, S. Iijima, Science 306 (2004) 1362.
[18] C.H. Kiang, J. Chem. Phys. 113 (2000) 4763.
[19] G.G. Tibbetts, J. Cryst. Growth 66 (1984) 632.
[20] M. Yudasaka, R. Yamada, N. Sensui, T. Wilkins, T. Ichihashi, S. Iijima, J. Phys. Chem. B 103 (1999) 6224.
[21] A.N. Andriotis, M. Menou, G. Frandakis, Phys. Rev. Lett. 85 (2000) 3193.
[22] H.T. Ng, B. Chen, J.E. Koehne, A.M. Cassell, J. Li, J. Han, M. Meyyappan, J. Phys. Chem. B 107 (2003) 8484.
[23] H.M. Christen, A.A. Puretzky, H. Cui, K. Belay, P.H. Fleming, D.B. Geohegan, Nano Lett. 4 (2004) 1939.
[24] B. Chen, G. Parker, J. Han, M. Meyyappan, A.M. Cassell, Chem. Mater. 14 (2002) 1891.
[25] I.A. Kinloch, M.S. Shaffer, Y.M. Lam, A.H. Windle, Carbon 42 (2004) 101.
[26] A. Bianco, K. Kostarelos, M. Prato, Curr. Opin. Chem. Biol. 9 (2005) 674.
[27] A. Kasuya, Y. Sasaki, Phys. Rev. Lett. 78 (1997) 4434.